Structure-based forest biomass from fusion of radar and hyperspectral observations

Robert N. Treuhaft
Jet Propulsion Laboratory, California Institute of Technology, USA

Gregory P. Asner
Department of Global Ecology, Carnegie Institution of Washington, Stanford University, USA

Beverly E. Law
College of Forestry, Oregon State University, USA

Received 30 December 2002; revised 21 February 2003; accepted 5 March 2003; published 8 May 2003.

[1] Forest biomass was estimated from the remotely sensed profiles of leaf area density. Biomass estimated from forest structure profiles may be more accurate than that determined from microwave power or optical radiance measurements. Multialtitude, airborne, C-band, radar interferometry produced relative density profiles, which were normalized by leaf area indices from airborne hyperspectral optical imagery, yielding the forest canopy leaf area density for 11 structurally diverse stands in Central Oregon. Fits of field biomass measurements to model functions of remotely sensed leaf area density produced agreement between the field and remotely sensed biomasses at the level of 25 tons/ha, or 16% of the average stand biomass. The errors in the field and remote sensing observations indicated that this level of agreement was significant with greater than 99.5% confidence. These results suggest that further demonstrations may lead to a set of model functions that enable global, structure-based biomass remote sensing. *INDEX TERMS:* 1615 Global Change: Biogeochemical processes (4805); 1640 Global Change: Remote sensing; 1694 Global Change: Instruments and techniques.
Citation: Treuhaft, R. N., G. P. Asner, and B. E. Law, Structure-based forest biomass from fusion of radar and hyperspectral observations, *Geophys. Res. Lett.*, *30*(9), 1472, doi:10.1029/2002GL016857, 2003.

1. Remote Sensing of Biomass Via Forest Structure

[2] Measurements of forest biomass are central to understanding carbon sequestration and change resulting from natural and anthropogenic processes. Balancing the terrestrial carbon budget, as well as detecting changes in land-use patterns, calls for global remote sensing of forest biomass. Global monitoring, in turn, requires model functions or algorithms, F, which transform a set of remote sensing observations into biomass, schematically represented as:

$$\text{Biomass}_{\text{rs}} = F(\text{Remote Sensing Observations};\ a, b, c \ldots), \quad (1)$$

The model function determining remotely sensed biomass, $\text{Biomass}_{\text{rs}}$, depends on parameters a, b, c.... A long-range goal necessary for global biomass remote sensing is to determine model functions, including associated parameters, either *a priori* or from remote sensing data, for all regions of interest around the globe. However, current demonstrations determine F using field measurements, estimating a, b, c... by minimizing the difference, in a least squares sense [*Hamilton*, 1964], between $\text{Biomass}_{\text{rs}}$ and field biomass measurements, $\text{Biomass}_{\text{f}}$, for a set of "training" stands.

[3] Until remote sensing of 3-dimensional forest structure became possible via radar interferometry [*Treuhaft et al.*, 1996; *Treuhaft and Siqueira*, 2000; *Reigber and Moreira*, 2000] and lidar [*Lefsky et al.*, 1999; *Drake et al.*, 2002], relationships like (1) often derived remotely sensed biomass from microwave power [*Moghaddam et al.*, 1994; *Dobson et al.*, 1995; *Luckman et al.*, 1997; *Paloscia et al.*, 1999] or optical radiance [*Sader et al.*, 1989; *Wu and Strahler*, 1994; *Steininger*, 2000]. Accuracies of these approaches, which are generally worse than the desired 10–20% (10–40 tons/hectare (ha) for most stands), in part reflect the radar and optical "saturation" phenomenon. When saturation occurs, radar power and optical reflectance generate biomass estimates with large errors, particularly at large biomass values. Additionally, for a given power or reflectance, biomass depends strongly on the vertical distribution of vegetation, as can be demonstrated from simple scattering and empirical considerations [*Imhoff*, 1995; *Treuhaft et al.*, 1996; *Steininger*, 2000]. Biomass estimates can erroneously span values corresponding to the range of unmeasured vertical structures. Structure measurements enable a new generation of model functions, which describe the physical apportioning of vegetation volume. They may therefore be simpler, accurate, robust, and may lead to the long-range goal of global biomass remote sensing.

2. Remotely Sensed Leaf Area Density

[4] In this demonstration, multialtitude, airborne C-band radar interferometry generated relative density profiles, which were constrained to be Gaussian. Hyperspectral optical observations yielded the one-sided leaf area index (LAI), which normalized the radar relative profiles to produce the leaf area density (LAD), as detailed in *Treuhaft et al.*, 2002. Our version of F first generates the biophysical vertical profile of LAD by performing a model-and-parameter-estimation process on the remote sensing observations, and from LAD the biomass is then estimated, as shown

0094-8276/03/2002GL016857$05.00

schematically in Figure 1. The goal of this paper is to gauge whether the accuracy and feasibility of using a remotely sensed biophysical vegetation profile to estimate biomass warrant pursuing this approach.

[5] The radar interferometric and hyperspectral optical data were taken over the Metolious River Basin in Central Oregon to produce remotely sensed LAD. LAI, tree dimensions, and biomass were measured in the field for 11 1-ha sites [*Law et al.*, 2001a, 2001b] to generate field estimates of LAD. These sites are diverse in species and successional stage, many containing predominantly ponderosa pine, others dominated by grand fir and larch. Some stands are a mix of mature and large old trees, where the mature trees exist at higher density, and are the first successful cohort following exclusion of fire for the past 100 years. Other stands are spatially uniform in age, and some contain sparse vegetation. These stands span a biomass range from 24–295 tons/ha, with a mean of 161 tons/ha.

[6] The NASA Airborne Synthetic Aperture Radar (AIRSAR) [*Zebker et al.*, 1992] and the Airborne Visible and Infrared Imaging Spectrometer (AVIRIS) [*Green et al.*, 1998] flew over a 20 × 10 km area in the spring and summer months of 1998, 1999, and 2000.

3. From Leaf Area Density to Biomass

[7] The general form of F relating the remotely sensed biomass to LAD in this paper is:

$$\mathrm{Biomass_{rs}} = F\left(\left\{\int LAD(z)f(z)dz\right\}; a, b\right). \qquad (2)$$

In (2), F involves a set of functions, $f(z)$, which weight LAD(z) in a set of integrals (denoted by {}) over the vertical coordinate z. Nonlinear least-squares approaches estimate two parameters a, b [*Hamilton*, 1964]. The observations and parameter-generated quantities are related by

$$\begin{pmatrix} \mathrm{Biomass_{f_1}} \\ \mathrm{Biomass_{f_2}} \ldots \\ \mathrm{Biomass_{f_N}} \\ \{\mathrm{z_{0_i}}\} \\ \{\sigma_\mathrm{i}\} \\ \{\mathrm{LAI_i}\} \end{pmatrix} = \begin{pmatrix} \mathrm{Biomass_{rs_1}}\left(\hat{z}_{0_1}, \hat{\sigma}_1, \hat{LAI}_1, a, b\right) \\ \mathrm{Biomass_{rs_2}}\left(\hat{z}_{0_2}, \hat{\sigma}_2, \hat{LAI}_2, a, b\right) \ldots \\ \mathrm{Biomass_{rs_N}}\left(\hat{z}_{0_N}, \hat{\sigma}_N, \hat{LAI}_N, a, b\right) \\ \{\hat{z}_{0_i}\} \\ \{\hat{\sigma}_i\} \\ \left\{\hat{LAI}_i\right\} \end{pmatrix} + \begin{pmatrix} \varepsilon_{\mathrm{f_1}} \\ \varepsilon_{\mathrm{f_2}} \ldots \\ \varepsilon_{\mathrm{f_N}} \\ \left\{\varepsilon_{z_{0_i}}\right\} \\ \{\varepsilon_{\sigma_i}\} \\ \{\varepsilon_{LAI_i}\} \end{pmatrix} \qquad (3)$$

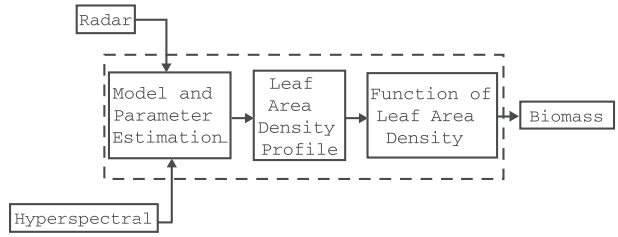

Figure 1. Schematic diagram of estimating biomass from radar and hyperspectral data via leaf area density. Leaf area density is produced by performing a model-and-parameter-estimation process on the remote sensing observations. The dashed box contains F of (1).

where field biomass for stand i is $\mathrm{Biomass_{f_i}}$, and $\varepsilon_{\mathrm{f_i}}$ is the field biomass measurement error. Below the field biomasses in the observation vector on the left are the remote sensing observations z_{0_i}, the location of the Gaussian peak of LAD, σ_i, the Gaussian standard deviation, and $\mathrm{LAI_i}$, the remotely sensed leaf area index, as explained in *Treuhaft et al.*, 2002. Parameters in the vector to the right of the equal sign, corresponding to each of the remote sensing structural observations and indicated with hats, are estimates of the actual remote sensing observations, given their errors and the fit suggested by (3). These parameters are used to calculate the model Gaussian LADs and biomasses, explicitly shown in (4a). Allowing estimates of these remote sensing parameters to shift away from the observations, constrained by the remote sensing observation errors $\varepsilon_{z_{0_i}}$, ε_{σ_i}, ε_{LAI_i} in the error vector, is a way of accounting for those errors, and is an important component of assessing the performance of variants of F [*Bierman*, 1977]. Minimizing the difference between the observations to the left of the equal sign and the quantities in the vector to the right, in a least-squares sense, yields all the parameter estimates. Values of LAI observations in (3) ranged from 0.3 to 5.7, and the LAI observation errors from hyperspectral data were about 5–10%. Radar observations of Gaussian peak locations ranged from 0 to 24 m, while Gaussian standard deviations were between 0.4 and 20 m. Errors on the radar structure parameters generating LAD were typically in the 1–2 meter range.

[8] Demonstrating the feasibility of the approach in (2) entails finding a model function F which, when the parameters in (3) are estimated, brings the reduced χ^2 (χ^2 per degree of freedom) close to unity [*Hamilton*, 1964] and produces an RMS difference between the field and remotely sensed biomasses that is in the 10–40 tons/ha range. Four trial LAD model functions, (4a) through (4d), were used to estimate the parameters in (3). The resulting RMS differences between field and remote sensing biomasses and reduced χ^2s are in Table 1 for each trial F. The first three model functions, (4a) through (4c), were simple functions of LAD involving its total integral, LAI, its standard deviation, σ_{z_i}, and its mean, $\bar{z}_i$. The fourth variant of F, chosen on the basis of inspection of the remote sensing LADs and the field biomasses, depends on all of the LAD-related quantities in (4a), (4b), and (4c). The 4 structure-based trial functions, plus one additional involving C-band radar power for the i^{th} stand, p_i, (for completeness), are

$$\text{Biomass}_{\text{rs}_i} = a + b\int LAD_i(z)\,dz = a + b\int_0^\infty \left[\frac{\hat{LAI}_i\,\exp\left(\frac{-\left(z-\hat{z}_{0_i}\right)^2}{2\hat{\sigma}_i^2}\right)}{\int_0^\infty \exp\left(\frac{-\left(z-\hat{z}_{0_i}\right)^2}{2\hat{\sigma}_i^2}dz\right)}\right]dz = a + b\,\hat{LAI}_i \quad (4a)$$

$$\text{Biomass}_{\text{rs}_i} = a + b\sqrt{\frac{\int LAD_i(z)\,z^2dz}{\int LAD_i(z)\,dz} - \left(\frac{\int LAD_i(z)\,z\,dz}{\int LAD_i(z)\,dz}\right)^2} \equiv a + b\sigma_{z_i} \quad (4b)$$

$$\text{Biomass}_{\text{rs}_i} = a + b\frac{\int LAD_i(z)z\,dZ}{LAI_i} \equiv a + b\bar{z}_i \quad (4c)$$

$$\text{Biomass}_{\text{rs}_i} = a + b\left[\sqrt{LAI_i \times \int LAD_i(z)\,z^2dz - \left(\int LAD_i(z)\,zdz\right)^2} + \frac{\int LAD_i(z)\,zdz}{LAI_i}\right] \equiv a + b[LAI_i\,\sigma_{z_i} + \bar{z}_i] \quad (4d)$$

$$\text{Biomass}_{\text{rs}_i} = a + bp_i. \quad (4e)$$

[9] Figure 2 shows the field-measured biomass for the 11 stands in Central Oregon versus the remotely sensed biomass, as determined by adjusted parameters using the best performing model function (4d). The RMS scatter of remotely sensed biomass about field biomass is 25 tons/ha The high and improbable value of 2.0 for the reduced χ^2 of even the best relation (4d) suggests either the need for refinement of (4d) or reassessment of the field or remote sensing errors, increasing them by about 40% [*Hamilton*, 1964]. Monte Carlo simulations with random noise for the remote sensing observations show that, given the field and remote sensing errors, the RMS scatter and reduced χ^2 for (4d) could be realized serendipitously only 0.5% of the time, confirming a 99.5% confidence on the significance of the performance of (4d).

4. Prognosis for Global Structure-Based Biomass Measurements

[10] The results of this paper indicate that the aggregate accuracy of relation (4d) and the field and remote sensing measurements is approximately 25 tons/ha, or 16% of the mean values observed in the field. These results suggest that, in order to isolate the accuracy of relations like (4d), additional higher accuracy structure-based demonstrations should focus on different regions of the Earth, spanning diverse forest vegetation types. Future demonstrations will also rely on lidar profiling [*Drake et al.*, 2002], which, when fused with radar interferometric and hyperspectral observations [*Slatton et al.*, 2001], may produce the most robust, global vegetation structure measurements. The best model function in this study (4d) may not be optimal for different forest species, climates, or topographic settings. Ideally, a generic set of model functions of forest structure will be determined to enable global remote sensing of biomass. Ultimately, structure measurements may play a role in specifying model functions *and* their parameters(a and b in this study). Other data, such as topographic or spectroscopic measurements beyond LAI, may also contribute to model function specification, enabling true remote sensing by minimizing the need for extensive field measurements.

Table 1. RMS Scatters and Reduced χ^2 for (4a)–(4e)

Biomass relation to Remote Sensing Data	RMS Scatter (tons/ha)	Reduced χ^2
4a) a + b LAI	75	7.4
4b) a + b σ_z	35	4.4
4c) a + b $\bar{z}$	131	27.7
4d) a + b[LAI $\sigma_z + \bar{z}$]	25	2.0
4e) a + b p	48	1.6

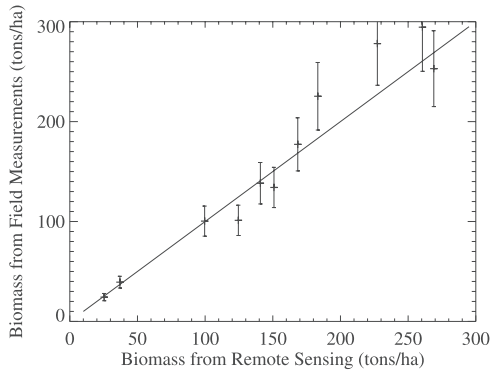

Figure 2. Field-measured biomass versus biomass from microwave and hyperspectral remote sensing using relation (4d). The RMS scatter of the remotely sensed biomass about the field-measured biomass is 25 tons/ha. The reduced χ^2 is 2.0.

[11] **Acknowledgments.** We thank S. van Tuyl for acquisition and analysis of field data. We also thank David Imel and the AIRSAR team, and Robert Green and the AVIRIS team for data acquisition and processing, as well as Mark Smith and Paul Siquiera for ground-based AIRSAR support. This work was supported by NASA OES grant NAG5-8320 (RTOP 622-93-63-40). G. Asner was also supported by NASA New Millenium Program grant NAG5-5253. The research described in this paper was carried out in part by the Jet Propulsion Laboratory, California Institute of Technology, under contract with the National Aeronautics and Space Administration. This is CIW Department of Global Ecology publication 027.

References

Bierman, G. J., *Factorization Methods for Discrete Sequential Estimation*, Academic Press, Orlando, 1977.

Dobson, M. C., F. T. Ulaby, L. E. Pierce, T. L. Sharik, K. M. Bergen, J. Kellndorfer, J. R. Kendra, E. Li, C. Lin, A. Nashashibi, K. Sarabandi, and P. Siqueira, Estimation of forest biophysical characteristics in Northern Michigan with SIR-C/X-SAR, *IEEE Trans. Geosci. and Rem. Sens.*, *33*(4), 877–892, 1995.

Drake, J. B., R. O. Dubayaha, D. B. Clark, R. G. Knoxd, J. B. Blair, M. A. Hofton, R. L. Chazdon, J. F. Weishampel, and S. D. Prince, Estimation of tropical forest structural characteristics using large-footprint lidar, *Remote Sensing of Environment*, *79*, 305–319, 2002.

Green, R. O., M. L. Eastwood, and O. Williams, Imaging spectroscopy and the Airborne Visible/Infrared Imaging Spectrometer (AVIRIS), *Rem. Sens. Environ.*, *65*, 227–240, 1998.

Hamilton, W. C., *Statistics in Physical Science: Estimation, Hypothesis Testing, and Least Squares*, Ronald Press, New York, 1964.

Imhoff, M. L., A theoretical analysis of the effect of forest structure on synthetic aperture radar backscatter and the remote sensing of biomass, *IEEE Trans. Geosci. and Rem. Sens.*, *33*(2), 341–352, 1995.

Law, B. E., S. Van Tuyl, A. Cescatti, and D. D. Baldocchi, Estimation of leaf area index in open-canopy ponderosa pine forests at different successional stages and management regimes in Oregon, *Agricultural and Forest Meteorology*, *108*, 1–14, 2001a.

Law, B. E., A. Cescatti, and D. D. Baldocchi, Leaf area distribution and radiative transfer in open-canopy forests: Implications to mass and energy exchange, *Tree Physiology*, *21*, 777–787, 2001b.

Lefsky, M. A., W. B. Cohen, S. A. Acker, G. G. Parker, T. A. Spies, and D. Harding, Lidar remote sensing of the canopy structure and biophysical properties of Douglas-Fir Western Hemlock forests, *Remote Sens. Environ.*, *70*, 339–361, 1999.

Luckman, A., J. Baker, T. M. Kuplich, C. F. Yanasse, and A. C. Frery, A study of the relationship between radar backscatter and regenerating tropical forest biomass for spaceborne SAR instruments, *Rem. Sens. Of Environment*, *60*, 1–13, 1997.

Moghaddam, M., S. Durden, and H. Zebker, Radar measurement of forested areas during OTTER, *Rem. Sens. Of Environment*, *47*, 154–166, 1994.

Paloscia, S., G. Macelloni, P. Pampaloni, and S. Sigismondi, The potential of C- and L-band SAR in estimating vegetation biomass: the ERS-1 and JERS-1 experiments, *IEEE Trans. Geosci. and Rem. Sensing*, *37*(4), 2107–2110, 1999.

Reigber, A., and A. Moreira, First demonstration of airborne SAR tomography using multibaseline L-band data, *IEEE Trans. Geosci. and Rem. Sensing*, *38*(5), 2142–2152, 2000.

Sader, S. A., R. B. Wade, W. T. Lawrence, and A. T. Joyce, Tropical forest biomass and successsional age class relationships to a vegetation index derived from Landsat TM data, *Rem. Sens. Of Environment*, *28*, 143–156, 1989.

Slatton, K. C., M. M. Crawford, and B. L. and Evans, Fusing interferometric radar and laser altimeter data to estimate surface topography and vegetation heights, *IEEE Trans. Geosci. and Rem. Sensing*, *39*(11), 2470–2482, 2001.

Steininger, M. K., Satellite estimation of tropical secondary forest aboveground biomass: data from Brazil and Bolivia, *Int. J. Remote Sensing*, *21*(6&7), 1139–1157, 2000.

Treuhaft, R. N., G. P. Asner, B. E. Law, and S. Van Tuyl, Forest leaf area density profiles from the quantitative fusion of radar and hyperspectral data, *J. Geophys. Res.*, *107*(D21), 4568–4578, 2002.

Treuhaft, R. N., and P. R. Siqueira, Vertical structure of vegetated land surfaces from interferometric and polarimetric radar, *Radio Sci.*, *35*, 141–177, 2000.

Treuhaft, R. N., S. N. Madsen, M. Moghaddam, and J. J. van Zyl, Vegetation characteristics and underlying topography from interferometric radar, *Radio Sci.*, *31*, 1449–1485, 1996.

Wu, Y., and A. H. Strahler, Remote estimation of crown size, stand density, and biomass on the Oregon transect, *Ecological Applications*, *4*(2), 299–312, 1994.

Zebker, H. A., S. N. Madsen, J. Martin, K. B. Wheeler, T. Miller, Y. Lou, G. Alberti, S. Vetrella, and A. Cucci, The TOPSAR interferometric radar topographic mapping instrument, *IEEE Trans. Geosci. Remote Sensing*, *30*, 933–940, 1992.

Gregory P. Asner, Department of Global Ecology, Carnegie Institution of Washington, Stanford University, Stanford, CA 94305, USA.

Beverly E. Law, 328 Richardson Hall, College of Forestry, Oregon State University, Corvalis, OR 97331, USA.

Robert N. Treuhaft, Jet Propulsion Laboratory, California Institute of Technology, 4800 Oak Grove Drive, MS138-212, Pasadena, CA 91109, USA.